http://dx.doi.org/10.21611/qirt.1992.013

Infrared thermography characterization of Görtler vortex type patterns in hypersonic flows

by D. BOSCHER (*), B. BAUDOUY (*), A. DEOM (*), M.-C. COET (**), J. DELERY (**) and D. BALAGEAS (*)

(*) Thermophysics Division, (**) Aerodynamics Department
ONERA , BP 72 F-92322 Châtillon-Cedex, France.

Abstract

The spanwise modulation of the heat transfer occuring, in hypersonic, on a two-dimensional compression ramp following a flat plate (Görtler vortices type structures) has been studied using infrared thermography. The technique allows a quantitative analysis. In particular, parameters like the relative amplitude of the heat transfer coefficient (h) modulation, amplitude of the local recovery temperature (T_r)
92 modulation, spatial frequencies of theses modulations were obtained from the time-resolved thermography of the model surface. The two modulations (h and T_r) are in phase opposition, fact until now unexplained.

Nomenclature

b	effusivity ($J\,m^{-2}\,s^{-1/2}\,K^{-1}$)	To	initial wall temperature (K)
c	volume heat capacity ($J\,m^{-3}\,K^{-1}$	Tr	recovery temperature (K)
h	convect. heat transfer coeff. ($W\,m^{-2}\,K^{-1}$)	T	T wall temperature (K)
k	thermal conductivity ($W\,m^{-1}\,K^{-1}$)	t	time (s)
		ϕ	heat flux ($W.m^{-2}$)

1. Introduction

For many years, infrared thermography has been in common use in wind tunnels for localizing areas where the transition between laminar and turbulent regimes takes place [1]. Progresses achieved in the technology of infrared scanners permit now the determination with a good precision of transient wall-temperature distribution on models in wind tunnels. The combination of this technique with heat transfer analysis and modelling allows to determine quantitatively the distribution of heat transfer coefficients [2].

We shall present here results obtained using this technique, concerning the aerothermal analysis of the phenomena which take place in the reattachment zone of a ramp, in hypersonic.

2. Interaction phenomena on a hypersonic ramp

The deflection produced by a control surface (flap, elevon) on a hypersonic vehicle is at the origin of a shock wave leading to a strong interaction with the boundary layer which develops on the vehicle. If this deflection goes beyond a limit value, the intensity of the shock can become such that it induces separation of the boundary layer. Then a rather complex flow establishes itself in the vicinity of the control surface. The boundary layer separates at a point which can be located well upstream of the hinge line. Downstream, a shear layer, well detached from the wall, develops. In most situations, this shear layer reattaches on the control surface at the reattachment point.

The separation phenomena leads to very typical wall pressure and wall heat transfer distributions whose features depend on the nature - laminar or turbulent - of the incoming

http://dx.doi.org/10.21611/qirt.1992.013

boundary layer. The distribution of heat transfer in the interaction region is important for practical applications. Considering a laminar boundary layer, separation itself is accompanied by a small decrease in heat transfer. This decrease is followed by a sharp increase in the reattachment region, the heat transfer value reaching a peak at a short distance downstream of the reattachement point. For a turbulent initial boundary layer, a slight rise in heat transfer occurs at separation and the peak at the reattachment can be more than ten times higher than for a laminar boundary layer. The phenomenon, which is accompanied by a spanwise modulation of the heat transfer, leads to heating effects which can be well in excess of those existing at the blunted nose of the vehicle. Thus, prediction of the heat transfer distribution on a control surface, or on any part of the vehicle where separation is likely to occur, is of crucial importance for the proper sizing of thermal protections.

Basic experiments on this problem are classicaly performed by considering a simplified geometry most often constituted by a flat plate - with sharp or rounded leading edge - followed by a rectilinear ramp representing the control surface.

3. Infrared thermographic setup and software

A long-wave monodetector camera (AGEMA 782) has been used for the present tests. For data acquisition and storage, real time digitizing was chosen. This solution offers very good signal-to-noise ratios. The digitizing hardware is capable of supporting tests of long duration (which is not the case in the present experiments for which duration is between 5 to 7 s) and is easily transportable. The system, called PTR-9010®, was developed under ANVAR grant, in cooperation with the CEDIP Company and under ONERA licence. It is based on a Compaq 386 microcomputer carrying a high-speed access 680-Mbyte formatted hard disk and a safeguard unit (WORM of 2x325 Mbyte). Two specific boards were developed to digitize and store the images in real time, and these were integrated into the microcomputer. The central RAM can hold all of the images (6.25 four-raster images/s, each containing 256 lines of 250 points digitized in 12 bits). The recordable time is then, limited to a few seconds. For longer duration tests, the data is stored in real time on the disk, with two possibilities: either one out of two images with 256 points per line or all of the images but with only 125 points per line.

Software tools exist to generate a synthetic overall view of the test, but also to obtain fine analyses of certain sequences and print out clear, readable documents. The program is user-friendly, accessible by menu and is able to sort out rapidly what is of interest for analysis. In particular, the software is able to provide the following functions: (i) dynamic viewing of the test by presentation of all of the rasters in store, in rapid succession, (ii) display of several rasters at the same time, for easier comparison and to detect variations, (iii) filtering/smoothing if necessary, (iv) identification of model elements in the infrared image, (v) converting radiance images to temperature images, (vi) converting temperature images to convective flux or heat transfer coefficient images, and (vii) extraction of time-varying thermograms at particular points on the model.

Furthermore, the system also offers the possibility of performing active thermography. Thus the microcomputer can control a unit of radiant energy power directed on the model. A schematic diagram of the system is given in *figure 1*.

4. Calculation of convective heat fluxes ans heat transfer coefficients

From the time variation of the model surface temperature distribution, convective heat fluxes and heat transfer coefficients have to be deduced. The advantage of the thermographic technique is mainly the possibility of elaborating 2-D or 3-D inverse methods, once the whole surface distribution is known. In fact, we shall consider here 1-D problems, each pixel being considered as thermally independent of the others. The 2-D and 3-D refinements are always possible but they are time consuming and not necessary in the present case.

http://dx.doi.org/10.21611/qirt.1992.013

The models here considered being poor conductors of heat, the thermal modelling is based on the semi-infinite medium assumption. The flux, at every moment can be deduced from the thermogram $T(t)$ by the classical integral formula:

$$\phi(t) = b/\sqrt{\pi}\,[(\,T(t)-To) / \sqrt{t} + 0{,}5 \int_0^t [T(t)-T(\tau)] / (t-\tau)^{3/2}\, d\tau\,] \qquad (1)$$

in which ϕ is the density of the heat flux at the surface and b the effusivity of the material the surface is made of ($b = \sqrt{k}\sqrt{c}$, k being the heat conductivity and c the heat capacity per unit volume). If the recovery temperature, $Tr(t)$, is known, the heat-transfer coefficient h is then found from the flux and from the thermogram by the expression:

$$h = \phi(t) / [Tr(t)-T(t)] \qquad (2)$$

IIf the recovery temperature is unknown and varies slowly, the heat-transfer coefficient can be found by taking the derivative of the flux:

$$h = -\,\partial\phi / \partial T \qquad (3)$$

and the recovery temperature can be found by the relation:

$$Tr(t) = T(t) + \phi(t)/h. \qquad (4)$$

5. Test arrangement

The tests were performed in the hypersonic wind tunnel R3Ch of the ONERA's Chalais-Meudon Center. All results were obtained with the following flow conditions: upstream Mach number : 10, stagnation pressure : 125 bars, total temperature : 1040 K, Reynolds number for the caracteristical length of the model (0,25 m from the leading edge to the hinge line) equal to 2.1 x10^6.

Figure 2 presents the schematic diagram of the set-up. The model, a flat plate with a metallic sharp leading edge followed by a 15° angle ramp, is made of Norcoat 4000 ®, a material currently used for thermosensitive paint tests.

The camera, with a 7°x7° or 12°x12° objective, is placed in a pressurized vessel and an extra lens can be positionned between the camera and the model to obtain a smaller field of view, when a better spatial resolution is needed. *Figure A** presents the temperature distribution on the ramp, showing clearly a structure made of streaks that is sometimes related to Görtler vortices. The interest of the smaller field is obvious.

6. Data reduction

The quality of the measurements appears on *figure 3*, where the temperature-time history of a given pixel is shown. The signal-to-noise ratio is good enough for there to be little noise in the heat flux-time history. Using the formula (1), from the evolution of the wall temperature, the heat flux entering the wall, ϕ_{cond}, can be deduced. It is necessary to take into account the radiation flux emitted by the wall, ϕ_{rad}, to deduce the convective heat flux :

$$\phi_{conv}(t) = \phi_{cond}(t) + \phi_{rad}(t)$$

Thanks to the low conductivity of the material used for the present model (Norcoat ® 4000 material), the wall temperature during the test reaches values not too far from the recovery temperature. Thus, it is possible to deduce the heat transfer coefficient without considering the recovery temperature. *Figure 4* presents the convective heat flux for a given pixel as a function of the local wall temperature. The linear variation allows the identification of this coefficient (slope of the curve) and of the true local recovery temperature (abscissa at the origin). The same

* *The colour plates of this article* **13** *are located on page* **III** *of the colour gathering, at the end of the book*

http://dx.doi.org/10.21611/qirt.1992.013

operation performed for each pixel yields the heat transfer coefficient image (left) and local recovery temperature image (right) of the *figure B*.

7. Analysis of the heat transfer coefficient and local recovery temperature distribution

From the two images of the *figure B* we can extract longitudinal distributions of h and Tr. From the heat transfer coefficient, and using the free stream conditions (density, velocity and theoretical recovery temperature) the Stanton number distribution is obtained (see *figure 5*). From the *h* distribution which is in relatively good agreement with previously published results from thermocouple measurements [3], the transitional nature of the flow is confirmed (the sharp increase of the heat transfer in the reattachment zone being much higher than for a fully laminar interaction). Similar longitudinal distributions are obtained for the local recovery temperature. They present slighter variations at the beginning of the ramp and a plateau at the rear part (see *figure 6*). At the beginning of the ramp, there is a large difference between the theoretical recovery temperature calculated for the flat plate and the experimental one, which is much lower than predicted.

The lateral distributions of *h* and *Tr,* taken from the two images of plate *B*, present modulation as expected. This modulation is not regular and it appears that several spatial frequencies are co-existing. This fact was quantitatively demonstrated by operating, line by line, a Fourier transform of the thermographic images. With the large-field of view, the spectral analysis reveals various space periods from the full field to some millimeters. A maximum of amplitude is obtained in particular for a space period of 7.3 mm, which may correspond to the vortices qualitatively seen on the images of *figure B*. This particular spatial period is identified with better accuracy and signal to noise ratio from the small field image. The striation typical period is 6.7 mm, value close to that identified in the large field image.

In fact, one can suppose that the interaction analyzed is disturbed by the irregular transition occurring on the model, which can be related to the variability of the surface state and the surface geometry of the sharp leading edge. An attempt of an experimental demonstration of such relation was recently made by SIMEONIDES (*et al.)*[4]. Thus the observed field seems to be the superimposition of this phenomenon and of a more regular pattern centered on the 6.7 mm spatial period.

Now, if we consider both lateral modulations (*h* and *Tr*), an interesting fact appears : these two modulations are in phase opposition, i.e. a maximum of *Tr* occurs when a minimum of h is obtained, and reciprocally. This is demonstrated in *figure 7*, where the following normalized parameters, plotted as functions of the lateral abscissa, are compared : (*h*-240)/120 and (740-*Tr*)/90. With this normalization, the two distributions are identical. This is particularly true when considering small spatial periods (smaller than 50 mm on this graph). For the large periods, which could correspond to the transition phenomena, a unique normalization does not lead to such a good agreement.

8. Conclusion

The infrared thermography was used for analyzing the reattachment zone on a flap at Mach 10. The method, thanks to the tremendous amount of informations delivered, allowed to show several interesting phenomena until now not displayed. The main results of this short series of tests are the followings .

i) The spanwise modulation of the heat transfer on the ramp could be due to the conjunction of two phenomena : the laminar to turbulent transition and the occurrence of vortices in the reattachment zone.

http://dx.doi.org/10.21611/qirt.1992.013

ii) The transition induces modulations characterized by erratic large space periods and large amplitudes. The space periods, which seems related to the surface and geometric quality of the leading edge, range from some tens of mm to the full width of the model.

iii) The modulations induced by the vortices are more regular, and characterized by smaller space periods, one of which seeming predominant and equal to 6.7 millimeters in our configuration. The amplitudes of these modulations are rather limited and near of ten per cent of the total heat transfer.

iv) The heat flux modulation is due to concomitant modulation of the heat transfer coefficient and of the local recovery temperature. On a large part of the ramp, this last parameter is much smaller than the theoretical recovery temperature.

v) The two modulations, heat transfer coefficient and recovery temperature, are in phase opposition, i.e. a maximum of heat transfer coefficient occurs when a minimum of recovery temperature is obtained, and reciprocally. The physical explanation of this phenomena remains to be found, in relation with the vortices presence. If we can suppose that the maximum of heat transfer is located in downwash regions (see *figure 8*), the variation of local recovery temperature is not so obvious.

REFERENCES

[1] GARTENBERG (E.) and ROBERTS (S.) Jr. - *Twenty-five years of aerodynamic research with infrared imaging*, in Thermosense XIII, SPIE Proc. vol. 1467, 1991, p. 338-353.

[2] BALAGEAS (D.L.), BOSCHER (D.M.) and DEOM (A.A.). - *Measurement of convective heat transfer coefficients on a wind-tunnel model by passive and stimulated infrared thermography,* in Infrared Technology XVI, SPIE Proc. vol. 1341, 1990, p. 339-357.

[3] DELERY (J.) and COET (M.-C.). - *Experimentation on shock wave/boundary layer interactions produced by two-dimensional ramps and three-dimensional obstacles.* Workshop on Hypersonic Flows for Reentry Problems, Antibes, January 22-26 1990.

[4] SIMEONIDES (G.), VERMEULEN (J.P.), BOERRIGTER (H.L.) and WENDT (J.F.) . *Quantitative heat transfer measurements in hypersonic wind tunnels by means of infrared thermography.* Von Karman Institute preprint 1991-29/AR.

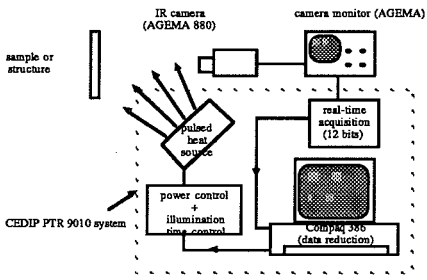

Fig. 1 - Schematic diagram of the Cedip-Onera PTR 9010® System used for both passive and active IR hermography in ONERA wind tunnels.

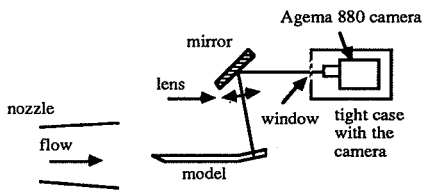

Fig 2. - Test configuration in ONERA's R3 Ch wind-tunnel for heat transfer measurements on a ramp.

http://dx.doi.org/10.21611/qirt.1992.013

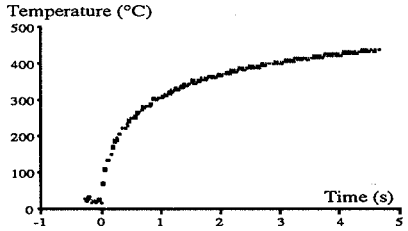

Fig. 3. - Temperature-time history of a given pixel extracted from the series of temperature images (at absc. x = 35 mm from the beginning of the ramp

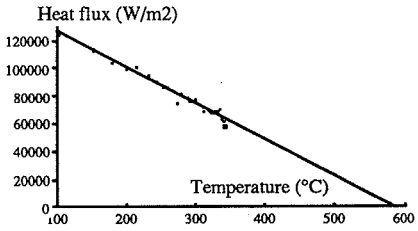

Fig. 4. - Measured convective heat flux as a function of the local wall temperature for a given pixel at x = 35mm.

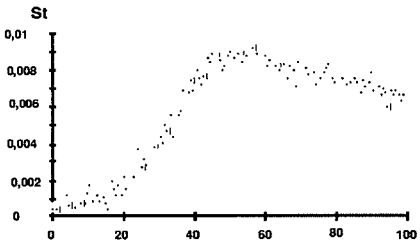

Fig. 5. - Longitudinal distribution of Stanton number n the reattachment zone at location z = 185 m

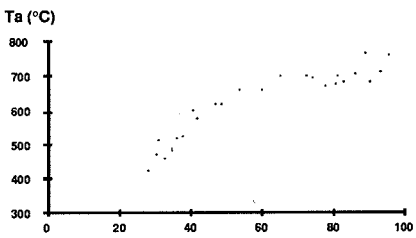

Fig. 6 - Longitudinal distribution of local recovery temperature in the reattachment zone at z = 185 mm.

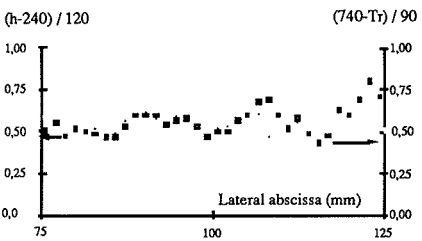

Fig. 7. - Demonstration of the phase opposition of *h* and *Tr* lateral modulations,using normalizations.

F

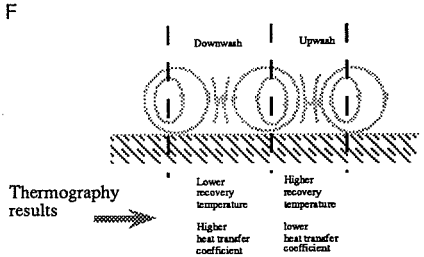

Fig. 8. - A possible configuration of the vortices and the wall heating spanwise modulation.